

Hydrothermal Synthesis of Copper Sulfide Flowers and Nanorods for Lithium-Ion Battery Applications

Shurui Yang¹, Yan Ran¹,
Huimin Wu¹,
Shiquan Wang^{1*},
Chuanqi Feng¹ and
Guohua Li²

Abstract

Copper sulfide flowers and nanorods were prepared by a surfactant-assisted hydrothermal process, using copper chloride and thiourea or thioacetamide as reactant in the presence of polyethylene glycol (PEG). The influences of sulfurating reagents and reaction temperatures on the morphologies of CuS particles are investigated. The microstructures and morphologies of as-prepared CuS were characterized by using powder X-ray diffraction (XRD), scanning electron microscopy (SEM), transmission electron microscopy (TEM), and energy-dispersive X-ray analysis (EDX), respectively. The morphologies of CuS prepared with thiourea are mainly flower-like, but the morphologies of CuS prepared with thioacetamide are nanorods and microtubes under the same reaction conditions. Due to the stability of structure, the CuS prepared with thiourea presents better cyclability compared to the CuS prepared with thioacetamide. The results reveal that sulfur sources and reaction temperature play important roles on controlling the morphologies and electrochemical performance of CuS particles as cathode materials for lithium ion batteries (LIBs). The CuS synthesized with thiourea at 140°C shows a highest discharge capacity (the first capacity is 187.1 mAh g⁻¹ and 71.72 mAh g⁻¹ after 50 cycles) at 30 mA g⁻¹ current density at room temperature in the range of 1.8-2.6 V.

Keywords: Hydrothermal synthesis; Copper sulfide; Nanostructures; Cathode materials; Lithium-ion batteries

Received: October 29, 2018; **Accepted:** October 30, 2018; **Published:** December 31, 2018

Introduction

Copper sulfide is a good prospective optoelectronic material, which is often used for LED, photocatalyst, and electrochemical cell [1-6]. Copper sulfide has also been used for artificial rainfall agent. For these applications, a variety of techniques [7-15], such as sonochemical synthesis [16], microwave [17], hydrothermal process [15], and solvothermal synthesis [18] have been developed to prepare copper sulfide with controllable microstructures, morphologies such as particles, rods, wires, flakes, disks, snowflake, flowerlike structures, or hollow spheres, etc. For example, Cao et al. [19] reported that shape-controlled synthesis of CuS nanorods, nanoflakes, and flowerlike structures had been achieved simply in the presence of a nonionic surfactant polyethylene glycol (PEG 20000) by adjusting hydrothermal temperature. Li et al. [20] reported that CuS nanomaterials with hierarchical structures were produced by solvothermal method. Mehdi Mousavi-Kamazani et al. [21] reported the

successful synthesis of various copper sulfide nanostructures via coprecipitation and hydrothermal routes. Azam Sobhani et al. [22] reported that CuS nanocrystals were synthesized via hydrothermal decomposition of [bis(thiosemicarbazide) copper (II)] without any surfactant. Masoud Salavati-Niasari et al. [23] synthesized zinc sulfide (ZnS) nanoclusters via the reaction between a new precursor, bis(salicylaldiminato) zinc (II); [Zn(sal)₂]; and thioacetamide (CH₃CSNH₂). The results show that different reaction conditions such as reaction temperature, growth time and sulfur sources are crucial factors on the final morphology and size of CuS nanomaterials.

- 1 Ministry-of-Education Key Laboratory for Synthesis and Applications of Organic Functional Molecules, Hubei Collaborative Innovation Center for Advanced Organic, Chemical Materials, Hubei University, Wuhan, P.R. China
- 2 School of Chemical Engineering and Materials Science, Zhejiang University of Technology, Hangzhou, P.R. China

***Corresponding author:**
Shiquan Wang

✉ wsqhao@hubu.edu.cn

Ministry-of-Education Key Laboratory for Synthesis and Applications of Organic Functional Molecules, Hubei Collaborative Innovation Center for Advanced Organic, Chemical Materials, Hubei University, Wuhan 430062, P.R. China.

Tel: +86 27 88662747

Citation: Yang S, Ran Y, Wu H, Wang S, Feng C, et al. (2018) Hydrothermal Synthesis of Copper Sulfide Flowers and Nanorods for Lithium-Ion Battery Applications. J Nanosci Nanotechnol Res Vol.2 No.2:7

CuS has a good electronic conductivity of $10^{-3} \text{ S}\cdot\text{cm}^{-1}$ and a high energy capacity of $\sim 560 \text{ mAh}\cdot\text{g}^{-1}$ and flat charge/discharge plateaus. Many papers reported that CuS was investigated as anode material for lithium ion battery (LIB) [24,25], only very few attempts have been made to use CuS as a cathode material for rechargeable lithium battery [26-29]. This is due to the main problem of a rapid drop in capacity and the formation of electrolyte soluble Li_2S during the course of the reaction [30,31]. Hughes et al. [26] stated that the main problem of the Li/CuS secondary cell was a rapid drop in capacity. Exner and Hep [27] reported that a Li/CuS coin cell with a 1M $\text{LiCF}_3\text{SO}_3/1, 3$ -dioxolane electrolyte gave only 50% charge capacity compared with the discharge capacity at a constant current. Chung et al. [29] reported the electrochemical behaviors of high purity CuS powers as a cathode material for lithium secondary batteries performed in 1M LiPF_6/EC -2 EMC electrolyte. High purity CuS could undergo a two-step reaction during the first discharge to 1.5 V with a capacity of 530 mAh g^{-1} , since impurities such as copper sulfates, copper thiosulfates, sulfur and moisture affected significantly the electrochemical performance of the CuS electrode [28,29]. The cyclability could be much improved by limiting the potential window between 2.6 and 1.8 V. The capacity was maintained of more than 70% of the initial value over 60 cycles. Nagarathinam et al. [32] reported the synthesis of hollow nanospheres and flowers of CuS and the electrochemical behavior of these nanosized CuS meso-assemblies as a cathode material for LIBs. Utilization of a novel two-dimensional coordination polymer generated from a trinuclear building block as a precursor in the synthesis of copper sulfide serendipitously resulted in CuS nanospheres with hollow interiors. It was revealed that the reaction proceeds through an insertion and deinsertion mechanism in the voltage window of 1.8-2.6 V at a current rate of 5 mA g^{-1} . There was a fading in storage capacity was observed for two CuS electrodes, especially for CuS electrode with a flower-like morphology. Though the first discharge capacity of hollow CuS spheres was found to be 400 mAh g^{-1} , the discharge capacity only maintained 75 mAh g^{-1} in the 40 cycles at a current rate of 5 mA g^{-1} . The results demonstrated that CuS with a hollow interior was more efficient and had good cyclability compared to that with a flower-like morphology. Chen et al. [33] reported the hydrothermal synthesis of copper sulfide with novel stick-like hierarchical structures and its application in LIBs. The usage of β -cyclodextrin was considered to be the first critical factor in controlling the morphologies. The first discharge capacity was only 94 mAh g^{-1} in the voltage range of 1.8-2.6 V at 0.2 C, but after 30 cycles, the discharge capacity remained 93 mAh g^{-1} . The as-prepared CuS exhibits excellent cycle stability, retaining capacity retention of 99% after 30 cycles.

Herein, CuS flowers and nanorods have been synthesized in the presence of a nonionic surfactant polymer, PEG-400, by a simple hydrothermal process using $\text{CuCl}_2\cdot 2\text{H}_2\text{O}$ and thiourea (NH_2CSNH_2 , Tu) or thioacetamide (CH_3CSNH_2 , TAA) as reactants at different temperatures (120°C , 140°C , 180°C , 200°C). It is found that the sulfurating reagents and reaction temperatures play important roles on controlling the morphologies and electrochemical performance of CuS particles as cathode materials for LIBs. Compared with other methods, the advantages of this method is that different sulfur sources can be used to prepare samples with

different morphologies. Meanwhile, a controllable synthesis can be applied to study the effects of different external conditions on the morphology of the products.

Materials and Methods

Preparation of CuS samples

All reagents were of analytical grade without further purification. In a typical procedure, 0.002 mol (0.341 g) of copper chloride ($\text{CuCl}_2\cdot 2\text{H}_2\text{O}$), 0.004 mol (0.304 g) of thiourea (H_2NCSNH_2) or 0.004 mol (0.30 g) of thioacetamide (CH_3CSNH_2) and 0.1 g of PEG ($M_n=400$, Aldrich) were dissolved into deionized water. Then the mixture was loaded into a 50 ml Teflon-lined stainless-steel autoclave and filled with deionized water up to 70% of the total volume. The autoclave was sealed and maintained at 120°C , 140°C for 24 h, and at 180°C and 200°C for 10 h without shaking or stirring during the heating period and then cooled to room temperature naturally. The black precipitates were filtered off and washed with distilled water and absolute ethanol. After dried in a vacuum at 60°C for 4 h, the final products were collected for characterization. Samples synthesized with thiourea and thioacetamide are designated as CuS-T-1 and CuS-T-2 ($T=120^\circ\text{C}$, 140°C , 180°C , 200°C), respectively.

Characterization

X-ray diffraction (XRD) pattern was obtained on a Bruker Advanced D8 X-ray diffractometer with Cu $K\alpha$ radiation ($\lambda=0.154 \text{ nm}$), using the step scanning, scanning speed is $5^\circ/\text{min}$; scanning range is 20° - 70° . The morphology of the products was examined using a Hitachi S-4800 scanning electron microscope (SEM) and a Tecnai G2 F30 transmission electron microscope (TEM). Energy-dispersive X-ray spectroscopy (EDX) was performed on an S-4800 scanning electron microscope.

Electrochemical measurements were carried out using a 2032-type coin cell fabricated in an argon-filled glove box (Mbraun, Germany). The working electrode was fabricated in the ratio of 70:20:10 (w/w) active material/carbon black/polyvinylidene difluoride (PVDF), while lithium foil served as counter and reference electrode. The electrolyte was 1 M LiPF_6 dissolved in 1:1 ethylene carbonate (EC) and dimethyl carbonate (DMC). Constant current charge/discharge cycling was conducted on a New ware battery tester in the voltage range between 2.6 and 1.8 V.

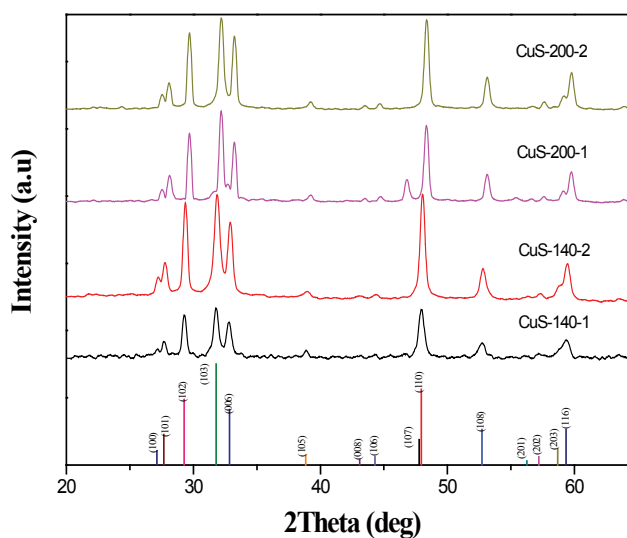
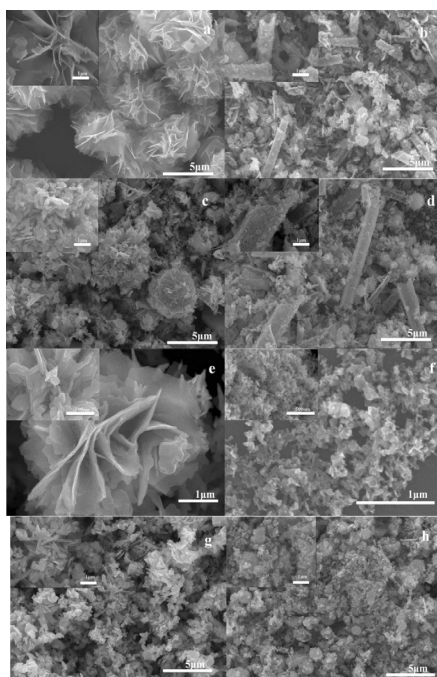
Results and Discussion

Hydrothermal reactions with Tu or TAA as the sulfurating reagent at different temperatures for 24 h or 10 h in an autoclave resulted in the formation of black products. The effects of sulfurating reagent, reaction temperature, and reaction time on the morphologies are shown in **Table 1**.

The typical XRD patterns of samples are shown in **Figure 1**. All diffraction lines can be indexed to the pure hexagonal CuS phase, which is in good agreement with the literature (JCPDS No. 06-0464). In Fig. 1, the presence of the (107) diffraction peak from

Table 1 The effects of preparation conditions on the morphologies of the products.

| Sample | Sulfur Source | Synthesis condition | Morphology |
|-----------|---------------|---------------------|-------------------------|
| CuS-120-1 | Tu | 120°C, 24 h | flowers |
| CuS-120-2 | TAA | 120°C, 24 h | Nanorods and microtubes |
| CuS-140-1 | Tu | 140°C, 24 h | Irregular flowers |
| CuS-140-2 | TAA | 140°C, 24 h | Nanorods and microtubes |
| CuS-180-1 | Tu | 180°C, 10 h | Irregular flowers |
| CuS-180-2 | TAA | 180°C, 10 h | Irregular particles |
| CuS-200-1 | Tu | 200°C, 10 h | Irregular flowers |
| CuS-200-2 | TAA | 200°C, 10 h | Irregular particles |

**Figure 1** Typical XRD patterns of the as-synthesized CuS samples, CuS-T-1 and CuS-T-2 (T=140°C, 200°C).**Figure 2** SEM images of CuS-T-1 and CuS-T-2 (T=120°C, 140°C, 180°C, 200°C). (a) CuS-120-1, (b) CuS-120-2, (c) CuS-140-1, (d) CuS-140-2, (e) CuS-180-1, (f) CuS-180-2, (g) CuS-200-1, (h) CuS-200-2, respectively. The inset of the each SEM image is the higher resolution SEM image.

the XRD patterns of CuS-T-1 ($T=200^{\circ}\text{C}$) may reflect that the growth direction of crystals along the (107) plane of sample CuS-T-1, which is not more obvious than that of sample CuS-T-2, which may have some relationships with the morphology of the resulting products [19]. The crystalline difference between CuS-T-1 and CuS-T-2 may be due to the different hydrolysis rate of H_2S from Tu and TAA during the hydrothermal process.

The morphologies of the as-prepared copper sulfide were characterized by SEM (**Figure 2**). The morphologies of CuS prepared with Tu and TAA as sulfur sources at the same reaction temperature are quite different, shown in **Table 1**. This is may be due to the formation rate of CuS particles because of different hydrolysis rate of Tu and TAA in water under the hydrothermal conditions. At lower hydrothermal temperatures (120°C), the CuS-T-1 takes on a hierarchal 3D flower-like morphology through self-assembly of nanoplates (**Figure 2a**). Using TAA as sulfur source instead of Tu, the as-obtained CuS shows nanorod-like structure with a diameter of 30 nm and the length of 50 nm. These nanorods can self-assemble into microtubes with a length of 2-5 μm (**Figure 2b**). As the reaction temperature increases, the morphologies of as-obtained CuS become random and irregular, as shown in **Figures 2c and 2d** (CuS-140-1 and CuS-140-2, respectively). The CuS-180-1 and CuS-200-1 take on irregular flower-like morphologies, with the thickness of plates of 100-200 nm (**Figures 2e-2g**). Meanwhile, the SEM images of CuS synthesized with TAA reveal that no microtubes can be found when the reaction temperature is above 180°C (**Figures 2f and 2h**) for CuS-180-2 and CuS-200-2). In high reaction temperature, the hydrolysis velocity of Tu and TAA change faster obviously so that the irregular CuS particles form before the CuS nanoparticles can self-assemble into flowers or microtubes.

The typical TEM images of the as-prepared CuS-120-1 and CuS-140-2 are shown in **Figure 3**. The nanoplate edges of CuS flower are seen in the low-magnification TEM image (**Figure 3a**), which reveals that the nanoplates with a thickness of ~ 30 nm have self-assembled into flowers. The presence of the hollow area in **Figure 3c** confirms that the CuS microtube is composed of nanorods with a diameter of ~ 30 nm and a length of ~ 200 nm. The interplanar spacing of the parallel fringes in the HRTEM images (**Figures 3b and 3d**) is 0.304 nm, which agrees well with the (102) plane of the hexagonal CuS. According to the Scherrer equation, $d=0.89\lambda/\beta\cos\theta$, where λ is the wavelength of X-ray radiation, θ the diffraction angle and β the full width at half maximum. The average values of d of the CuS are 29, 30, 33 and 32 nm for samples CuS-140-1, CuS-140-2, CuS-200-1 and CuS-200-2, respectively, which is close to the observation of the TEM or SEM images.

EDX analysis performed on the as-prepared CuS-180-1 sample (**Figure 4**) indicates that the flowers have a composition with Cu:S atomic ratio of 46:44, the silica peak comes from silica wafer supporting the sample. Taking into account the error of the measurement, the chemical formula of the flowers is close to CuS. Other samples have similar EDX results.

The typical N_2 adsorption analysis was measured to study the

specific surface area of the samples. N_2 adsorption isotherms **Figure 5**. From the adsorption branch of the isotherm, the specific surface area of CuS-140-1 and CuS-140-2 are $2.214\text{ m}^2\text{ g}^{-1}$ and $12.375\text{ m}^2\text{ g}^{-1}$, respectively.

The nucleation and growth mechanism of copper sulfide (CuS) is very complicated. Its shape, size and crystal form will vary greatly with different hydrothermal conditions. To the CuS-1, according to the previous literatures [34-36] and our results, the possible formation mechanism of copper sulfide (CuS) can be divided into three steps:

- The complex formed by thiourea with copper (II) ions will produce a large amount of CuS crystal nucleus under hydrothermal condition.
- CuS nucleus grow and form nanocrystals and nanosheets, generally.
- Nanoscaled CuS nanoplates directionally grow and then self-assemble into hierarchal 3D flower-like morphology.

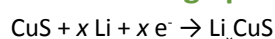
This is the following extrapolation combined with this experiment: thiourea and copper (ii) ion form $[\text{Cu}(\text{Tu})_n(\text{PEG})_m]^{2+}$ in aqueous solution, which is decomposed to form CuS nucleus and then form CuS microspheres with flower-like structure. The reactions may take the following form:

- $\text{Cu}^{2+} + n\text{Tu} + m\text{PEG} \rightarrow [\text{Cu}(\text{Tu})_n(\text{PEG})_m]^{2+}$ (1)
- $[\text{Cu}(\text{Tu})_n(\text{PEG})_m]^{2+} \rightarrow \text{CuS}$ (2)

To the CuS-2, the reaction mechanism may as follows: First, Cu^{2+} and CH_3CSNH_2 form $[\text{Cu}(\text{CH}_3\text{CSNH}_2)_2]^{2+}$. Then, the complex dissociates Cu^{2+} with the rise of temperature during hydrothermal process. Meanwhile, the thioacetamide hydrolyzes to form H_2S . Finally, Cu^{2+} ions and H_2S combine to form CuS nanorods or nanoparticles.

The use of CuS as a cathode material for LIB in liquid electrolyte is also investigated. **Figure 5** presents the typical charge/discharge curves of the CuS-140-1 samples during three cycles in the voltage window of 1.0-2.6 V at current rate of 30 mA g^{-1} . It can be seen that obvious discharging reactions take place at 2.07 V for CuS-140-1 and the electrochemical process during the first discharge is as shown below:

First discharge plateau reaction



The electrochemical behaviors of CuS-140-1 reported here during the first cycle are quite similar to those reported earlier on commercially available bulk CuS [29] and nanostructured CuS (hollow and flower-like) [32]. During the first discharge, the plateau at 2.07 V corresponds to the Li^+ insertion into the covellite CuS lattice forming a homogenous Li_xCuS phase [32]. Further research of insertion of lithium results in the conversion reaction as shown in the follow equation.

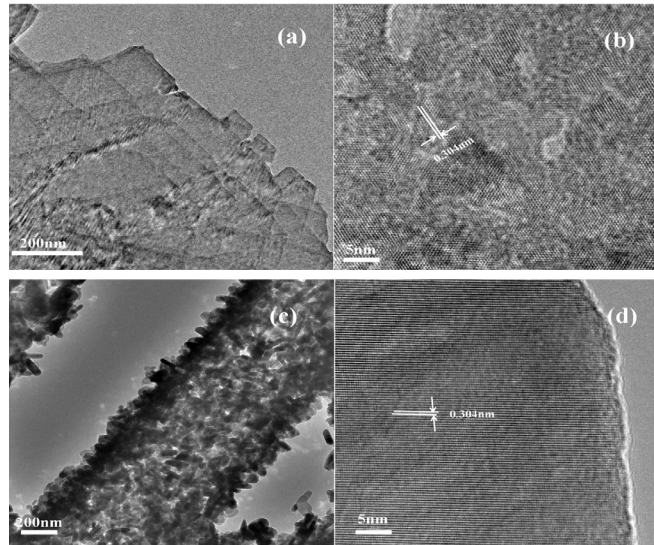


Figure 3 TEM and HRTEM images of (a and b) CuS-120-1 and (c and d) CuS-140-2.

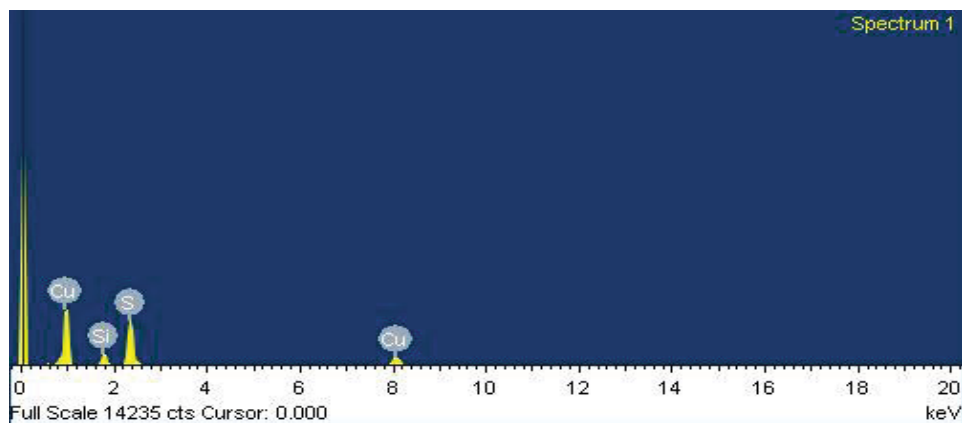


Figure 4 EDX results on CuS-180-1. The silica peak comes from silica wafer supporting the sample.

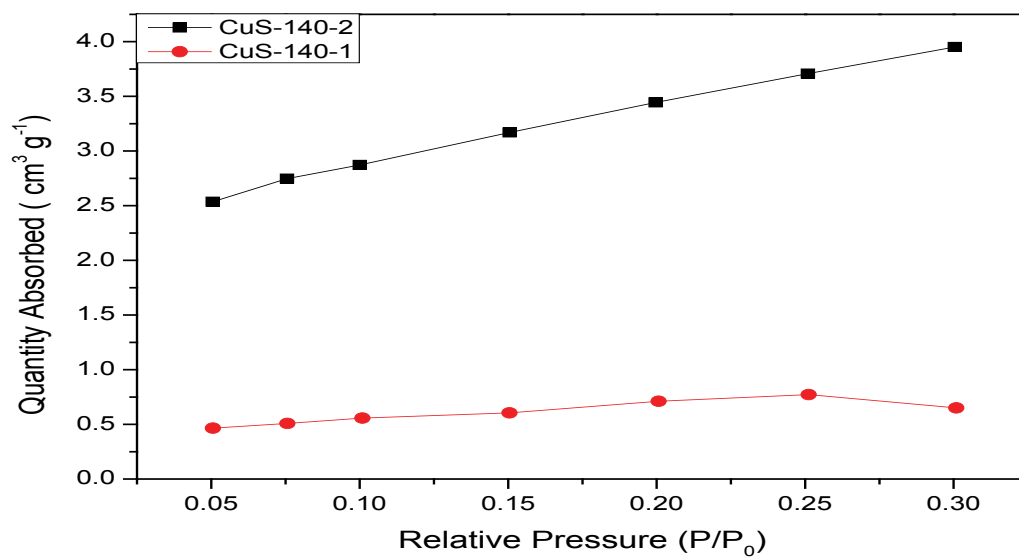
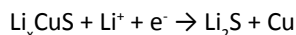


Figure 5 N₂ adsorption isotherms of CuS-140-1 and CuS-140-2.

Second discharge plateau reaction



Cu and Li_2S nanocomposite form during the reaction. Cycling within the potential window of 1.0-2.6 V causes drastic capacity fading within a few cycles due to the formation of Li_2S which is soluble in liquid electrolyte. Upon subsequent charging, considerable irreversible storage behavior has been noticed, due to the instability of nanosized Li_2S [32]. The above result shows that the discharge reaction consists of two-steps which correspond to two voltage plateau [29]. Overall, first discharge capacity of CuS-140-1 is found to be 397.9 mAh g^{-1} , which is 71.2% of the theoretical capacity of CuS. Second charging results in the plateau at 2.47 V, which corresponds to a capacity of 249.8 mAh g^{-1} , as shown in **Figure 6a**.

Figure 6b presents the first charge/discharge curves of the CuS samples in the voltage window of 1.8-2.6 V at current rate of 30 mA g^{-1} . If the potential range for cycling is limited between 2.6 and 1.8 V, it is expected that cyclability can be enhanced with high cycle efficiency. In general, the samples synthesized at higher hydrothermal temperatures show higher specific capacities in comparison with that synthesized at lower hydrothermal

temperatures. The samples prepared by Tu exhibit higher discharge capacities than that prepared by TAA at the same reaction conditions. Among these electrodes, the CuS-120-1 and CuS-120-2 electrodes show the first capacity is 133.5 mAh g^{-1} and 141.8 mAh g^{-1} . CuS-140-1 and CuS-140-2 electrodes exhibit a higher discharge capacity (the first capacity is 187.1 mAh g^{-1} and 173.8 mAh g^{-1} , respectively), as shown in **Figure 6b**. When the hydrothermal temperature is above 180°C , the as-obtained CuS samples (CuS-180-1, CuS-180-2, CuS-200-1, and CuS-200-2) electrodes exhibit the first discharge capacities of 136.1, 142.0, 173.6, and 169.5 mAh g^{-1} , respectively.

The electrochemical behavior of different CuS samples are presented at 30 mA g^{-1} up to 50 cycles, as shown in **Figure 7**. The samples synthesized at higher hydrothermal temperatures show higher specific capacities in comparison with that synthesized at lower hydrothermal temperatures, but their cyclabilities are not good. The samples prepared by Tu exhibit higher discharge capacities than that prepared by TAA at the same reaction conditions. It is found that CuS-T-1 ($T=140^\circ\text{C}$, 200°C) electrodes exhibit a higher discharge capacity (the first capacity is 187.1 mAh g^{-1} and 173.8 mAh g^{-1}), compared with the CuS-T-2 ($T=140^\circ\text{C}$, 200°C) electrodes. Interestingly, the CuS-120-1 electrode behaves excellent cyclability (first discharge capacity of $\sim 100 \text{ mAh g}^{-1}$

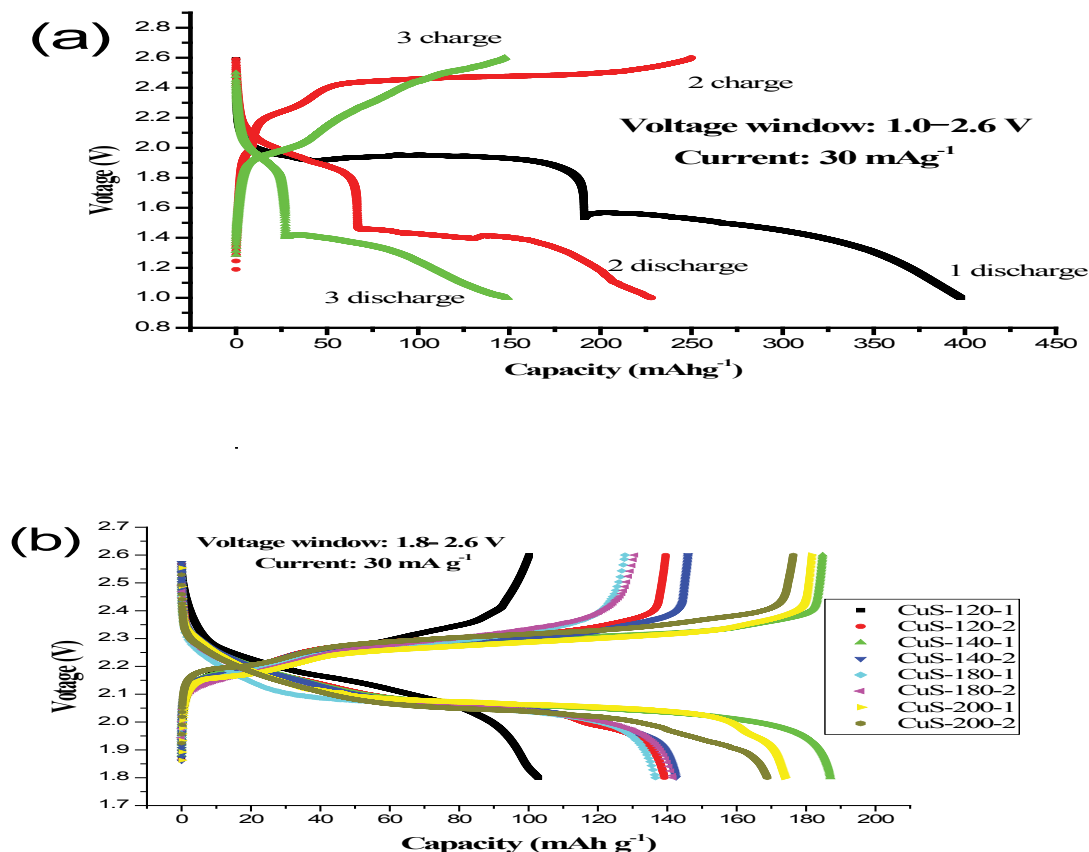


Figure 6 (a) Electrochemical behaviors of CuS-140-1 electrode during three cycles between 1.0 and 2.6 V range at room temperature; (b) The first discharge/charge curves of the CuS-T-1 and CuS-T-2 electrodes ($T=120^\circ\text{C}$, 140°C , 180°C , 200°C). Voltage range: 1.8-2.6 V, current density: 30 mA g^{-1} .

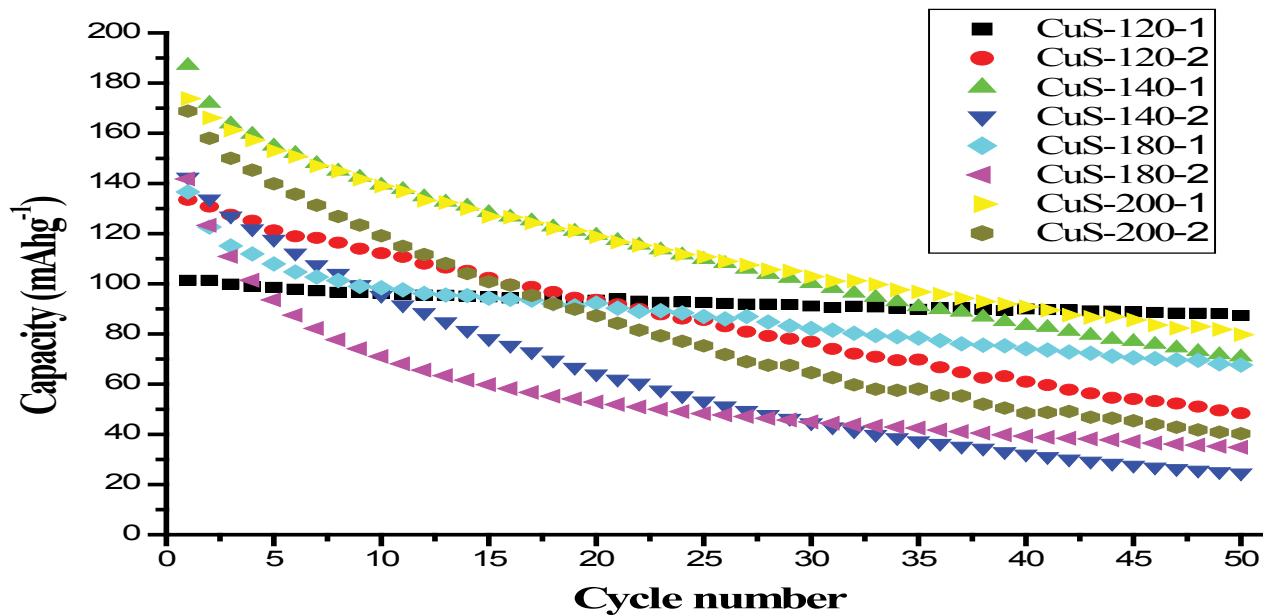


Figure 7 Cycling performance of the CuS-T-1 and CuS-T-2 electrodes ($T=120^{\circ}\text{C}$, 140°C , 180°C , 200°C). Voltage range: 1.8-2.6 V, current density: 30 mA g^{-1} .

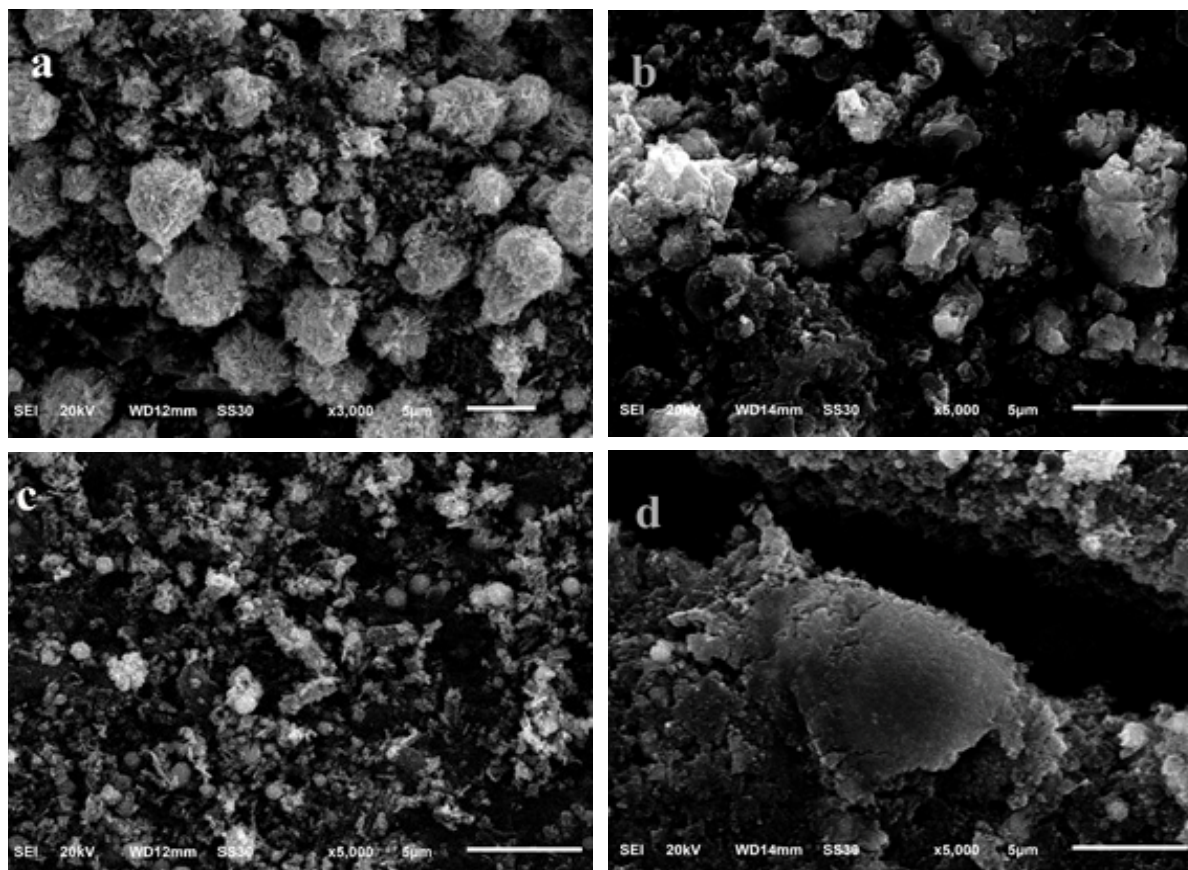


Figure 8 The SEM images: (a and c) the CuS-140-1 and CuS-140-2 before cycling; (b and d) the CuS-140-1 and CuS-140-2 after 20 cycles.

and 87.4 mAh g⁻¹ after 50 cycles). After 50 cycles, the discharge capacities of CuS-T-1 (T=140°C, 180°C, 200°C) electrodes drop to 71.72, 68.1, 79.7 mAh g⁻¹, respectively. The discharge capacities of CuS-T-2 (T=140°C, 180°C, 200°C) decrease to 25.18, 35.2 and 40.28 mAh g⁻¹, respectively. The improvement in the performance of CuS-T-1 (T=140°C, 180°C, 200°C) might be due to the stability of structure of CuS prepared with Tu as reactants. There are fading in discharge capacity for almost all, similar to the results of the hollow structured electrode material of CuS, due to the formation of Li₂S which is solvable in liquid electrolyte [32]. Current results demonstrate that as-prepared CuS flowers are more promising than the hollow CuS electrode [32] for LIB applications. The structure modification of CuS is needed to improve its cyclability and the related research is on the way.

In order to verify the structure change of the samples cycled after 20 cycles, SEM is employed to investigate the morphologies. Figures 8a and 8c are the SEM images of CuS-140-1 and CuS-140-2 before cycling, respectively. Figures 8b and 8d are the SEM images of CuS-140-1 and CuS-140-2 after cycling. Both the morphologies of CuS-140-1 and CuS-140-2 have profound changes after cycling. The micro flower morphology of CuS-140-1 has broken into particles (Figure 8b), which indicate that CuS have changed to the new substance, such as Cu, Li₂S, after the electrochemical reactions. Meanwhile, the CuS-140-2 nanorods also have changed dramatically. The cycled CuS-140-2 electrode

takes on the nanoparticle aggregation. The above phenomena can be ascribed to the insertion and desorption of lithium ion, which cause a formation of Cu and Li₂S and change in volume.

Conclusion

In summary, the synthesis of copper sulfide flowers and nanorods was realized by polymer-assisted hydrothermal process. It was found that different sulfur sources and reaction temperatures played important roles on controlling the morphologies of CuS particles and electrochemical performances. The morphologies of CuS prepared with TAA are nanorods and microtubes under the same reaction conditions. Though there are fading in discharge capacities, current results demonstrate that the as-prepared CuS flowers are more promising than CuS nanorods for LIB applications. Due to the stability of structure, the CuS flowers prepared with Tu presents a better cyclic stability compared to CuS nanorods prepared with TAA. The CuS synthesized with Tu at 120°C shows a best cyclability, the first capacity is ~100 mAh g⁻¹ and 87.4 mAh g⁻¹ after 50 cycles in the range of 1.8-2.6 V.

Acknowledgements

This work was financially supported by the Project of Hubei Provincial Science & Technology Department (No. 2018ACA147).

References

- 1 Nov IG, Najdoski M (1995) Optical and electrical properties of copper sulfide films of variable composition. *J Solid State Chem* 114: 469-475.
- 2 Nascu C, Pop I, Ionescu V, Indrea E, Bratu I (1997) Spray pyrolysis deposition of CuS thin films. *Mater. Lett* 32: 73-77.
- 3 Hermann AM, Fabick L (1983) Research on polycrystalline thin-film photovoltaic devices. *J Cryst Growth* 61: 658-664.
- 4 Wang M, Sun L, Fu X, Liao C, Yan C (2000) Synthesis and optical properties of ZnS:Cu(II) nanoparticles. *Solid State Commun* 115: 493-496.
- 5 Hu JQ, Deng B, Zhang WX, Tang KB, Qian YT (2001) A convenient hydrothermal route to mineral Ag₃CuS₂ nanorods. *Int J Inorg Mater* 3: 639-642.
- 6 Takase K, Koyano M, Shimizu T, Makihara K, Takahashi Y, et al. (2002) Electrical resistivity and photoluminescence spectrum of layered oxysulfide (LaO) CuS. *Solid State Commun* 123: 531-534.
- 7 Qiao ZP, Xie Y, Xu JG, Qian YT (1999) γ -Radiation synthesis of the nanocrystalline semiconductors PbS and CuS. *J Colloid Interface Sci* 214: 459-461.
- 8 Zhang Y, Qiao ZP, Chen XM (2002) Microwave-assisted elemental-direct-reaction route to nanocrystalline copper sulfides Cu₉S₈ and Cu₇S₄. *J Solid State Chem* 167: 249-253.
- 9 Wang H, Zhang JR, Zhao XN, Xu S, Zhu JJ (2002) Preparation of copper monosulfide and nickel monosulfide nanoparticles by sonochemical method. *Mater Lett* 55: 253-258.
- 10 Wang S, Yang S (2000) Surfactant-assisted growth of crystalline copper sulphide nanowire arrays. *Chem Phys Lett* 322: 567-571.
- 11 Wang S, Yang S (2001) Growth of crystalline Cu₂S nanowire arrays on copper surface: Effect of copper surface structure, reagent gas composition, and reaction temperature. *Chem Mater* 13: 4794-4799.
- 12 Chen J, Deng SZ, Xu NS, Wang S, Wen X, et al. (2002) Field emission from crystalline copper sulphide nanowire arrays. *Appl Phys Lett* 80: 3620-3622.
- 13 Chen X, Wang Z, Wang X, Zhang R, Liu X, et al. (2004) Synthesis of novel copper sulfide hollow spheres generated from copper (II)-thiourea complex. *J Cryst Growth* 263: 570-574.
- 14 Jiang CL, Zhang WQ, Zou G, Xu LQ, Yu W, et al. (2005) Hydrothermal fabrication of copper sulfide nanocones and nanobelts. *Mater Lett* 59: 1008-1011.
- 15 Lu Q, Gao F, Zhao D (2002) One-step synthesis and assembly of copper sulfide nanoparticles to nanowires, nanotubes, and nanovesicles by a simple organic amine-assisted hydrothermal process. *Nano Lett* 2: 725-758.
- 16 Kumar RV, Palchik O, Kolytyn Y, Diamant Y, Gedanken A (2002) Sonochemical synthesis and characterization of Ag₂S/PVA and CuS/PVA nanocomposite. *Ultrason Sonochem* 9: 65-70.
- 17 Liao XH, Chen NY, Xu S, Yang SB, Zhu JJ (2003) A microwave assisted heating method for the preparation of copper sulfide nanorods. *J Cryst Growth* 252: 593-598.
- 18 Liu J, Xue D (2009) Solvothermal synthesis of CuS semiconductor hollow spheres based on a bubble template route. *J Cryst Growth* 311: 500-503.
- 19 Ji H, Cao J, Feng J, Chang X, Ma X, et al. (2005) Fabrication of CuS

- nanocrystals with various morphologies in the presence of a nonionic surfactant. *Mater Lett* 59: 3169-3172.
- 20 Li F, Wu J, Qin Q, Li Z, Huang X (2010) Controllable synthesis, optical and photocatalytic properties of CuS nanomaterials with hierarchical structures. *Powder Technol* 198: 267-274.
- 21 Kamazani MM, Zarghami Z, Niasari MS (2016) Facile and novel chemical synthesis, characterization, and formation mechanism of copper sulfide (Cu_2S , $\text{Cu}_2\text{S}/\text{CuS}$, CuS) nanostructures for increasing the efficiency of solar cells. *The Journal of Physical Chemistry* 120: 2096-2108.
- 22 Sobhani A, Niasari MS, Mashkani SMH (2012) Single-source molecular precursor for synthesis of copper sulfide nanostructures. *J Clust Sci* 23: 1143-1151.
- 23 Niasari MS, Davar F, Mazaheri M (2009) Synthesis and characterization of ZnS nanoclusters via hydrothermal processing from [bis(salicylidene)zinc(II)]. *J Alloys Compd* 470: 502-506.
- 24 Wang Y, Zhang Y, Li H, Peng Y, Li J, et al. (2018) Realizing high reversible capacity: 3D intertwined CNTs inherently conductive network for CuS as an anode for lithium ion batteries. *Chem Eng J* 332: 49-56.
- 25 Ren Y, Wei H, Yang B, Wang J, Di J (2014) "Double-Sandwich-Like" CuS@reduced graphene oxide as an anode in lithium ion batteries with enhanced electrochemical performance. *Electrochimica Acta* 145: 193-200.
- 26 Hughes M, Hampson NA, Karunathilaka S (1984) A review of cells based on lithium negative electrodes (anodes). *J Power Sources* 12: 83-144.
- 27 Exner I, Hep J (1993) Copper (II) sulfide as cathode active materials in secondary lithium batteries. *J Power Sources* 44: 701-705.
- 28 Bredland AM, Messing TG, Paulson JW (1980) Proceeding of 29th power sources symposium of the electrochemical society, Pennington, New Jersey, pp: 82-85.
- 29 Chung JS, Sohn HJ (2002) Electrochemical behaviors of CuS as a cathode material for lithium secondary batteries. *J Power Sources* 108: 226-231.
- 30 Rauh RD (1979) A lithium/dissolved sulfur battery with an organic electrolyte. *J Electrochem Soc* 126: 523-527.
- 31 Peled E, Gorenshtein A, Segal M, Sternberg Y (1989) Rechargeable lithium-sulfur battery. *J Power Sources* 26: 269-271.
- 32 Nagarathinam M, Saravanan K, Leong WL, Balaya P, Vittal J (2009) Hollow nanospheres and flowers of CuS from self-assembled Cu (II) coordination polymer and hydrogen-bonded complexes of *N*-(2-Hydroxybenzyl)-L-serine. *Cryst Growth Des* 9: 4461-4470.
- 33 Chen GY, Wei ZY, Jin B, Zong XB, Wang H, et al. (2013) Hydrothermal synthesis of copper sulfide with novel hierarchical structures and its application in lithium-ion batteries. *Appl Surf Sci* 277: 268-271.
- 34 Jiang X, Xie Y, Lu J, He W, Zhu L, et al. (2000) Preparation and phase transformation of nanocrystalline copper sulfides (Cu_9S_8 , Cu_7S_4 and CuS) at low temperature. *J Mater Chem* 10: 2193-2196.
- 35 Han Y, Wang Y, Gao W, Wang Y, Jiao L, et al. (2011) Synthesis of novel CuS with hierarchical structures and its application in lithium-ion batteries. *Powder Technology* 212: 64-68.
- 36 Huang QL, Chen H, Zhang YC, Wu CL (2011) CuS nanostructures prepared by a hydrothermal method. *J Alloys Compd* 509: 6382-6387.